Solid State Communications 151 (2011) 425–429

Contents lists available at ScienceDirect

Solid State Communications

journal homepage: www.elsevier.com/locate/ssc

Possible coexistence of superconductivity and magnetism in intermetallic $NiBi_3$

Esmeralda Lizet Martinez Piñeiro [a], Brenda Lizette Ruiz Herrera [a], Roberto Escudero [a,*], Lauro Bucio [b]

[a] Instituto de Investigaciones en Materiales, Universidad Nacional Autónoma de México, A. Postal 70-360, México, D.F. 04510, Mexico

[b] Instituto de Física, Universidad Nacional Autónoma de México, México, D.F. 04510, Mexico

ARTICLE INFO

Article history:
Received 26 November 2010
Received in revised form
5 January 2011
Accepted 7 January 2011
by P. Chaddah
Available online 14 January 2011

Keywords:
A. Intermetallic alloys
D. Superconductivity
D. Ferromagnetism

ABSTRACT

$NiBi_3$ polycrystals were synthesized via a solid state method. X-ray diffraction analysis shows that the main phase present in the sample corresponds to $NiBi_3$ in a weight fraction of 96.82 % according to the refinement of the crystalline structure. SEM - EDS and XPS analysis reveal a homogeneous composition of $NiBi_3$, without Ni traces. The powder superconducting samples were studied by performing magnetic measurements. The superconducting transition temperature and critical magnetic fields were determined as $T_C = 4.05$ K, $H_{C1} = 110$ Oe and $H_{C2} = 3,620$ Oe. The superconducting parameters were $\xi_{GL} = 301.5$ Å, $\lambda_{GL} = 1549$ Å, and $\kappa = 5.136$. Isothermal measurements below the transition temperature show an anomalous behavior. Above the superconducting transition the compound presents ferromagnetic characteristics up to 750 K, well above the Ni Curie temperature.

1. Introduction

The coexistence of superconductivity and magnetism is a phenomenon of great interest in the scientific community. In 1957, Ginzburg [1] considered that the coexistence could exist if the critical field were longer that the induction created by the magnetization. Two years before the antagonistic nature of superconductivity and magnetism was confirmed when Matthias' experiments [2] showed that the superconductivity in lanthanum was destroyed by a small concentration of magnetic impurities. This was explained as in conventional *s*-wave superconductors, local magnetic moments break up spin singlet Cooper pairs and hence strongly suppress superconductivity, an effect known as magnetic pair-breaking. Because of the pair-breaking effect, in most superconductors the presence of only a 1% level of magnetic impurity can result in the almost complete destruction of the superconducting behavior.

The discovery of rare earth ternary and actinide compounds was the first opportunity to study the interaction between the magnetic moments of *f*-electrons and superconducting electrons in a very high density of local moments [3–5]. These compounds presented new exotic phenomena associated with the long-range order of local magnetic moments, such as reentrant superconductivity [6], coexistence of superconductivity and ferro-antiferromagnetism [7], magnetic field inducing superconductivity [8] and heavy fermion superconductivity [9].

$NiBi_3$ is an intermetallic alloy with an orthorhombic structure, $CaLiSi_2$-type and space group Pnma [10,11]. In this structure, bismuth atoms form an octahedral array, while nickel atoms form part of linear chains. $NiBi_3$ is a superconducting material with a critical temperature about 4.05 K [12], and is the object of study of this research.

Some initial studies has been done on the superconducting properties of $NiBi_3$. For instances Fujimori, et al. [13] have presented a study related to the superconducting and normal properties; they studied the resistivity, heat capacity, upper critical magnetic field, in polycrystals and needle-like single crystals.

Among the electronic characteristics of this intermetallic alloy is that it presents a large phonon resistivity due to predominant coupling of electrons by bismuth vibrations via the Ni vibrations. In this study we are mainly concerned with the magnetic-superconducting interacting effects, as we will discuss in the rest of the paper.

2. Experimental details

Several samples were studied. The preparation method for the most pure obtained sample was the following: the $NiBi_3$ composition was prepared by a solid state method using Bi pieces (Aldrich 99.999%) and Ni powder (Strem Chemicals 99.9%) in evacuated quartz tubes. The samples were melted in a resistance furnace at 1000 °C for seven days. The characterization was made by X-ray powder diffraction (XRD) (Bruker AXS D8 Advance) using Cu Kα radiation, scanning electron microscopy (SEM-EDS) (Leica-Cambridge), and X-ray photoelectron spectroscopy (XPS) (Microtech Multilab ESCA2000) using Al Kα radiation 1453.6 eV.

* Corresponding author. Tel.: +52 55 5622 4625.
E-mail address: escu@servidor.unam.mx (R. Escudero).

0038-1098/$ – see front matter © 2011 Elsevier Ltd. All rights reserved.
doi:10.1016/j.ssc.2011.01.005

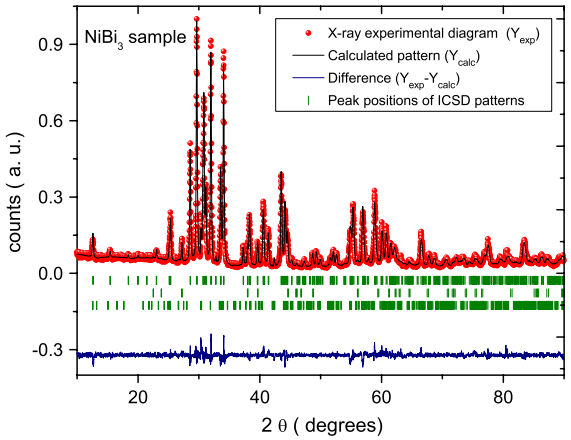

Fig. 1. (Color online) Rietveld refinement of $NiBi_3$ sample. Dots are the experimental data, the continuous line superposed on the dots is the calculated pattern. At the bottom of the diagram, the difference between the experimental and calculated points is shown. Vertical marks are displayed in three rows corresponding from top to bottom to the Bragg positions for the phase $NiBi_3$, Bi, and NiBi respectively.

The XPS spectra were obtained in the constant pass energy mode (CAE) $E_0 = 50$ and 20 eV for survey and high resolution respectively. The sample was etched for 20 min with Ar^+ at 3.5 kV during 20 min at 0.12 μA mm^{-2}. The peak binding energy (BE) positions were referenced to Au $4f_{7/2}$ at 84.00 eV and Ag $3d_{5/2}$ at 367.30 eV having a FWHM of 1.02 eV. Magnetization measurements and determination of the superconducting properties were performed using a Quantum Design (QD) superconducting quantum interference device (SQUID) MPMS system. We determined the transition temperature with magnetization versus temperature M(T) measurements with a small magnetic field about 10 Oe. Two normal distinct measuring modes were used, zero field cooling (ZFC) and field cooling (FC). Critical magnetic fields were determined by performing isothermal measurements $M(H)$ at different temperatures, from 2 to 4 K. We also performed isothermal measurements at different magnetic intensities at higher temperatures to observe possible magnetic behavior above the transition temperature and at much higher temperatures. In order to determine the Curie temperature and to discard the possibility of Ni as an impurity in the compound, we performed studies to observe in the isothermal curves, M–H, the existence of hysteresis, thus the coercive field at different temperatures, and well above the Ni and NiBi Curie temperatures using a Quantum Design oven installed in the MPMS.

3. Results and discussion

3.1. Structural characterization

The structural characterization determined by powder XRD and Rietveld refinement are shown in Fig. 1. The polycrystalline phases were identified by comparison with X-ray patterns in the Inorganic Crystal Structure Database (ICSD) 2010. All the peaks correspond to the $NiBi_3$ phase (ICSD 58821), except the weak peaks related to impurities of Bi (ICSD 64703) and NiBi (ICSD 107493), in a proportion less than 1% and 2% respectively. According to the results of the refinement, no Ni impurities were detected.

Refinement of the crystalline structure was performed using a Rietveld Fullprof program. Table 1 contains the $NiBi_3$ structural parameters, corresponding to the orthorhombic space group Pnma (62). In Fig. 2 is shown the crystalline structure.

Yoshida et al. [16] reported magnetic properties of NiBi. Unlike their samples with important amounts of nickel impurities, our $NiBi_3$ samples are completely free of nickel, according to the X-ray diffraction analysis, refinement, and XPS studies as we will show below.

Table 1
Crystallographic data for $NiBi_3$ obtained by Rietveld refinement starting with the structural parameters reported by Fjellvag and Furuseth [15] with symmetry described by the orthorhombic space group Pnma. The standard deviations are written between parentheses.

Rp (%)	Rwp (%)	Re (%)	χ^2 [14]
14.0	15.3	11.1	1.886
Parameters (Å)	$a = 8.879(1)$	$b = 4.0998(7)$	$c = 11.483(2)$
Volume (Å^3)	417.7(2)		
Site	x	y	z
Bi 1	0.298(3)	0.25	0.890(2)
Bi 2	0.382(4)	0.25	0.594(2)
Bi 3	0.409(3)	0.25	0.180(2)
Ni 1	0.09(1)	0.25	0.520(6)

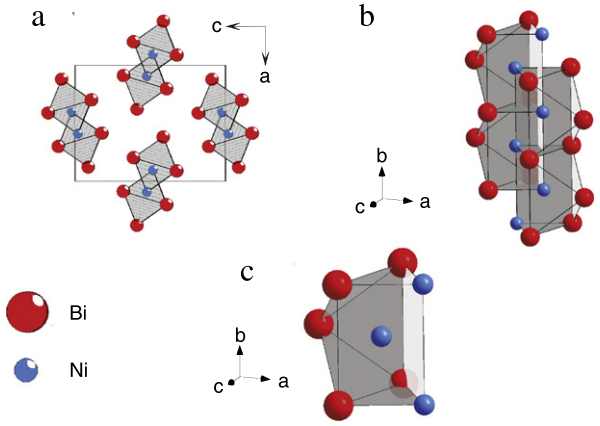

Fig. 2. (Color online) $NiBi_3$ crystalline structure. (A) Unit cell; (B) Rods of prisms oriented along the b axis; (C) Ni atoms with capped trigonal prismatic coordination and strong bonds Ni–Bi and Ni–Ni.

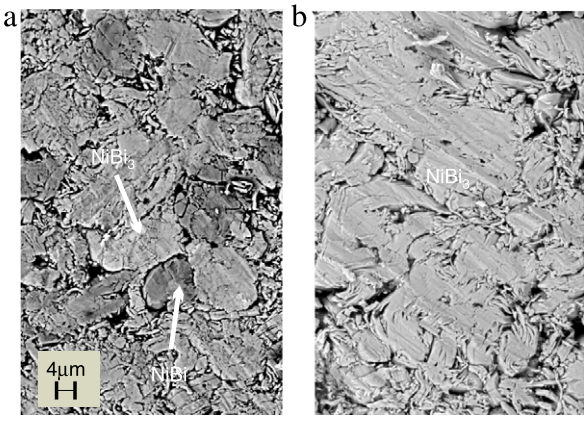

Fig. 3. SEM Images of $NiBi_3$. (a) $NiBi_3$ after heating at 1000 °C during 3 days, (b) and during 7 days.

Fig. 3 shows SEM-EDS images of $NiBi_3$. A comparison between two of our samples (a, b) with different reaction times; with three and seven days at 1000 °C are presented, respectively. Sample a shows the presence of two phases, NiBi and $NiBi_3$, differentiated by the color and borders clearly defined. Sample b shows a homogeneous composition of $NiBi_3$. Impurities of NiBi and Bi were not detected by EDS.

In order to discard nickel impurities, XPS analysis was performed in our samples. Fig. 4(a) shows the survey spectra for $NiBi_3$. It was observed that all peaks correspond to Ni and Bi, and no trace of other elements was found. Fig. 4(b) shows the XPS spectra at low binding energies for the $NiBi_3$ sample and its

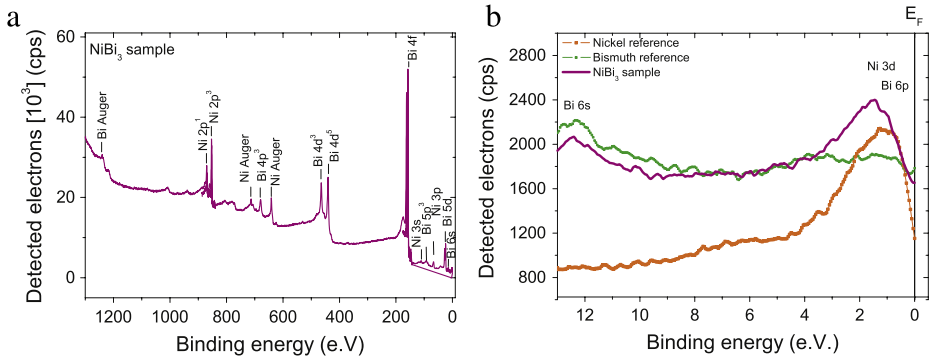

Fig. 4. (Color online) XPS analysis of $NiBi_3$. (a) XPS survey spectra for $NiBi_3$. (b) XPS valence band spectra for Ni, Bi, and $NiBi_3$.This XPS analysis shows that the compound is a phase without Ni impurities.

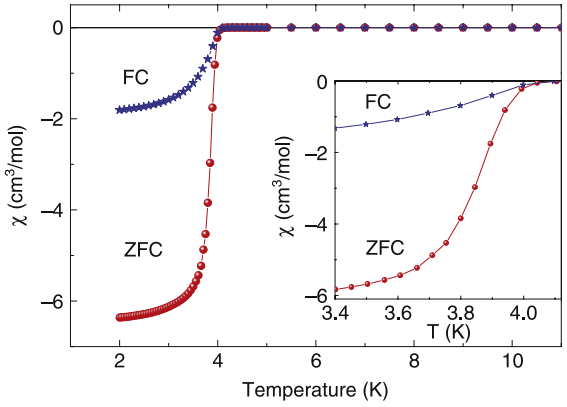

Fig. 5. (Color online) Shielding and Meissner fractions measured at 10 Oe. The inset displays the measurements close to the transition temperature. The onset of the transition is about 4.05 K.

comparison with bismuth and nickel metal references. The analysis of the sample in the valence region shows that the 3d peak of nickel spectrum displays an increasing width and movement to higher energies with respect to nickel metal. This effect is attributed to changes in the environment of the nickel atoms when forming part of the alloy, confirming that nickel atoms are part of the $NiBi_3$ compound and not an impurity.

3.2. Superconductivity

Magnetization measurements $M(T)$ performed in ZFC and FC modes were performed in order to determine the amount of superconducting fraction. The Meissner fraction of $NiBi_3$ sample was determined to be about 54.1% and was calculated a 2 K related to the maximum value $-4\pi\chi = -4\pi\rho$ M/mB, where ρ is the density of the material equal to 10.884 g/cm^3, M is the magnetization in emu, m is the mass in g, and B is the applied magnetic field [17]. The superconducting transition temperature T_C was 4.05 K and is defined as the point in which there is a drop in the susceptibility in the FC measurement. These results are shown in the Fig. 5.

3.3. Magnetic measurements

Magnetization measurements as a function of applied magnetic field $M(H)$, were used to calculate the superconducting parameters. The critical magnetic fields $H_{C1}(0)$ and $H_{C2}(0)$ were calculated from the experimental data and a linear fit using the expression $H_{Ci}(0) = -0.693T_C\ (\mathrm{d}H_{Ci}(T)/\mathrm{d}T\,|_{T=T_C})$ near T_C, where

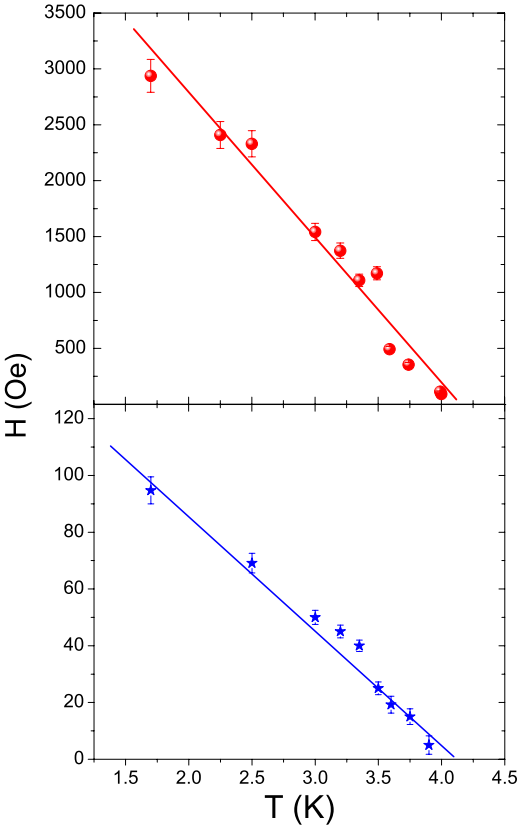

Fig. 6. (Color online) Critical fields H_{C1}, and H_{C2} as function of temperature. Critical fields were measured using isothermal magnetic curves, data were fit with the expressions mentioned in the main text.

$\mathrm{d}H_{Ci}(T)/\mathrm{d}T\,|_{T=T_C}$ corresponds to the slope of the linear fit [18]. Fig. 6 shows the critical magnetic fields.

The Ginzburg–Landau (GL) parameters; coherence length ξ_{GL}, penetration length λ_{GL}, κ, and the thermodynamical critical field $H_C(0)$, were estimated with the equations: $H_{C2}(0) = \phi_0/2\pi\xi_{GL}^2$, $H_{C2}(0)/H_{C1}(0) = 2\kappa^2/\ln\kappa$, $\kappa = \lambda_{GL}/\xi_{GL}$, and $H_C(0) = \phi_0/(2\sqrt{2}\pi\xi_{GL}\lambda_{GL})$ where ϕ_0 is the quantum flux. Also we may use $H_{C1}H_{C2} = H_C\ln\kappa$. The superconducting parameters are presented in Table 2 and are similar to the obtained by Fujimori, et al. [13].

3.4. Magnetic measurements below and above T_C

As was mentioned before different magnetic measurements were performed to have a better insight about the electronic properties of this alloy. Below the transition temperature $M(H)$

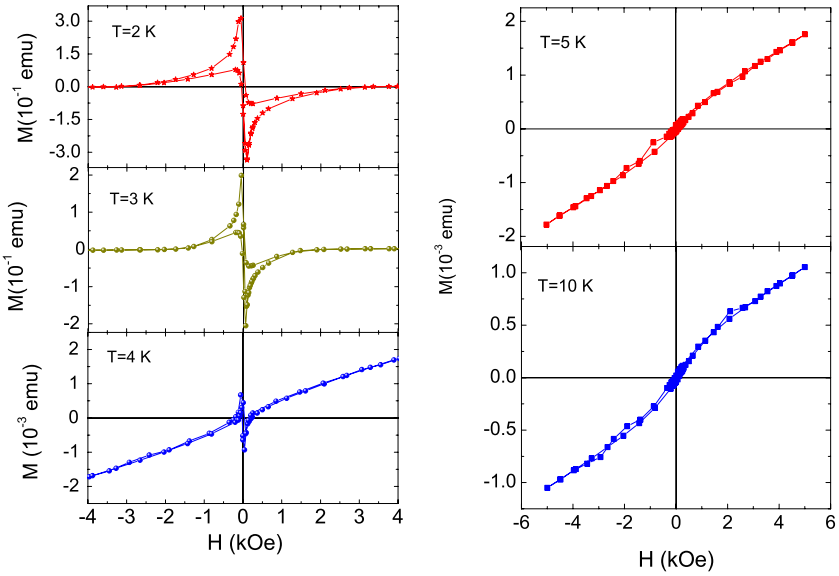

Fig. 7. (Color online) Isothermal magnetic measurements M–H in the superconducting region of $NiBi_3$, note the anomalous characteristics of the data, which is the effect of ferromagnetism in the sample.

Table 2
Superconducting parameters of $NiBi_3$ compound.

Property	Value
T_C	4.05±0.1 K
$dH_{C1}(T)/dT\|_{T=T_C}$	40±3 Oe/K
$dH_{C2}(T)/dT\|_{T=T_C}$	1290±80 Oe/K
$H_{C1}(0)$	110±8 Oe
$H_{C2}(0)$	3620±300 Oe
ξ_{GL}	302±10 Å
λ_{GL}	1549±100 Å
κ	5.1±0.2
$H_C(0)$	490±30 Oe

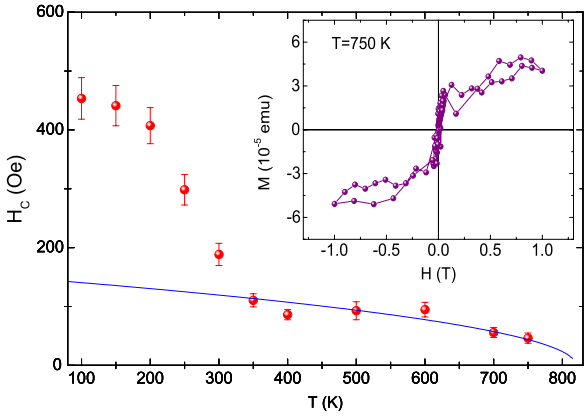

Fig. 8. (Color online) Coercive field extracted from M–H measurements from 100 to 750 K. Clearly a ferromagnetic behavior is observed, and also the coercive field. Accordingly the ferromagnetic transition is above 800 K, and consequently the only magnetic contribution is of $NiBi_3$. The inset shows the isothermal measurements at 750 K. At that temperature the ferromagnetic characteristic is still clearly observed at low fields.

measurements were used to determinate the critical fields in the usual manner; thus fitting a straight line to the $M(H)$ curve at different temperatures. Below T_C at the temperatures of 2, 3, and 4 K, Fig. 7 displays the competition between the diamagnetic characteristic of the superconducting state and the ferromagnetism of the compound. At low field $M(H)$ curves looks normal, so H_{C1} can be determined. However as soon as the maximum diamagnetism is reached, a fast decrease of the diamagnetic contribution, $-M$ is observed. This decreasing characteristic changes more rapidly that in normal superconductors (where the magnetism is absent). This anomalous behavior is the indication of two competing processes: superconductivity and ferromagnetism. At high temperature above the transition temperature, where the diamagnetic characteristic disappears, $M(H)$ shows a typically ferromagnetic characteristic; thus a tendency to saturation of the magnetization at high fields and a coercive field, h_C, at the central part of the curve.

$M(H)$ measurements were performed in order to determinate the coercive field h_C. We used a medium field model above the superconducting temperature given by: $h_C(T) = h_C(0)[1 - (T/\tau_C)^{1/2}]$, in this equation τ_C is the Curie temperature. In Fig. 8 we present the variations of h_C up to 750 K. The fitting line is the result of the above equation for h_C. At this high temperature we observed in the inset the $M(H)$ data obtained at 750 K. This last measurement is above the Curie temperature of Ni 355 °C (or 627 K [19]). The measurement performed at 750 K clearly indicates that $NiBi_3$ is the only magnetic contributing material. In the Yoshida's studies they observed that NiBi is magnetic at a maximum about 640 K. Our measurements show that at 750 K the coercive field is small and about 70 Oe.

4. Conclusions

We found that $NiBi_3$ is a type II superconducting material in which ferromagnetism and superconductivity coexist and present an interesting interplay. This is the first time that such a coexistence is demonstrated in a clear experimental manner. The ferromagnetic transition is persistent at very high temperatures about 750 K, well above the Curie temperature of Ni metal and the NiBi compound.

Acknowledgements

We thank F. Silvar for Helium provisions, Lazaro Huerta for the XPS measurements, Francisco M. Ascencio for his collaboration in the sample preparation.

References

[1] V.L. Ginzburg, Sov. Phys., JETP 4 (1957) 153.
[2] B. Matthias, H. Suhl, E. Corenzwit, Phys. Rev. Lett. 1 (1958) 449.
[3] S.L. Kakani, U.N. Upadhyaya, J. Low Temp. Phys. 70 (1988) 5.
[4] K Sinha, S.I. Kakani, Magnetic superconductors. Recent developments, Nova Science Publisher, inc., New York, 1989.
[5] H.R. Khan, C.J. Raub, Ann. Rev. Mater. Sci. 15 (1985) 211.
[6] M. Ishikawa, A.L. Fischer, Solid State Commun. 23 (1977) 37.
[7] H.C. Hamakar, et al., Solid State Commun. 31 (1979) 139.
[8] M.B. Maple, Physics Today 39 (1986) 72.
[9] F. Steglich, et al., Phys. Rev. Lett. 43 (1979) 1892.
[10] G.P. Vassilev, X.J. Liu, K. Ishida, J. Phase Equil. Diff. 26 (2005) 161.
[11] S. Park, K. Kangc, W. Hana, T. Vogt, J. Alloys Compd. 400 (2005) 88.
[12] N.E. Alekseevskii, N.B. Brandt, T.I. Kostina, Bull. Acad. Sci. URSS. 16 (1952) 233; J. Exp. Theor. Phys. 21 (1951) 951.
[13] Y Fujimori, Kan Sh-i, B Shinozaki, T. Kawaguti, J. Phys. Soc. Japan 69 (2000) 3017 and references there in.
[14] R.A. Young, The Rietveld Method, International Union of Crystallography, Oxford University Press, New York, 1993.
[15] H Fjellvag, S Furuseth, J. Less-Comm. Met. 128 (1987) 177.
[16] H. Yoshida, et al., Magn. Magn. Mater 239 (2002) 5.
[17] C.C. Lai, T.Y. Lin, Chin. J. Phys. 28 (1990) 4.
[18] L.F. Li, et al., Physica C 470 (2010) 313.
[19] C. Kittel, Introduction to Solid State Physics, 6th ed., John Wiley & Sons, Inc., New York, 1993.